Flow Through Very Porous Screens

Paul A. Durbin and
Kenneth K. Muramoto

NASA

Flow Through Very Porous Screens

Paul A. Durbin and
Kenneth K. Muramoto

Lewis Research Center
Cleveland, Ohio

Summary

An asymptotic analysis is done for flow through and around screens with small resistance coefficients. Both steady and oscillatory flows are considered, but only the case of a screen normal to the flow is treated. At second order in the asymptotic expansion the steady flow normal to the screen is nonuniform along the screen, due to components induced by the wake and by tangential drag. Therefore, the third-order pressure drop is nonuniform and the wake contains distributed vorticity, in addition to the vortex sheet along its boundary. The unsteady drag coefficient is found as a function of frequency.

Introduction

A two-dimensional screen of finite height, placed into an otherwise uniform flow, acts as a resistant surface so fluid can pass through the screen only if driven by a pressure drop. Fluid which passes around the screen will not suffer a resistive pressure drop so that, by Bernoulli's equation and continuity of pressure at the edge of the screen, it must have a higher velocity than the fluid in the wake. Hence, ideally the wake behind a screen is bounded by a vortex sheet (fig. 1). In general, vorticity will also be distributed throughout the wake.

The strength of the wake vortex sheet depends on the porosity of the screen, as modelled by screen resistance coefficients. In this report an analysis is done for screens with asymptotically small resistance. Only a uniform screen normal to the oncoming flow will be considered. It is found that the distributed wake vorticity is small, of third order, in the resistance coefficient.

An analysis of flow around a very porous screen was made by Taylor (ref. 1). He represented the screen by a sheet of sources whose strengths were chosen to give the appropriate pressure drop across the screen. Because he ignored flow induced by wake vorticity and effects of the sources within the sheet upon each other, Taylor's velocity field is formally accurate only to $O(k)$, where k is the small resistance coefficient of the screen. (By *formally accurate* we mean his approximation agrees with an exact asymptotic expansion to $O(k)$. However, Taylor did not expand his solution in powers of k. The form in which he expressed his drag coefficient agrees with experiment up to $k \approx 4$.)

Taylor's distributed source analysis was extended by Koo and James (ref. 2). They introduced a wake in an *ad hoc* fashion and ignored the flow in front of the screen induced by wake vorticity. Also, the inviscid condition that vorticity be a function of the stream function generally is not met by their model. Their model also produces spurious jumps of the tangential velocity across the screen and of the pressure across the wake boundary. All in all, Koo and James' model does not improve on the formal accuracy of Taylor's solution; however, it provides a good fit to data on drag coefficients (Graham, ref. 3). The present report is concerned more with the formal solution of governing equations than with robust modelling.

The **Approximate Analysis** section of this report describes an approach which agrees with the **Asymptotic Analysis** section (p. 4) to $O(k)$ in the velocity field. The approximate solution could be obtained by summing an infinite subset of terms in the formal asymptotic expansion; in the **Approximate Analysis** section the solution is derived by omitting the tangential drag on the screen and by ignoring the dynamical effect of wake vorticity. Thus, this approximation is analogous to Taylor's but, because it includes different higher order terms, it produces a different solution.

In the **Asymptotic Analysis** section a formal asymptotic expansion is carried out to $O(k^2)$. At this order effects of tangential drag and of wake vorticity have entered the solution, and the distributed wake vorticity is found.

In the **Unsteady Flow** section (p. 7) the drag coefficient of a screen in oscillatory uniform flow is calculated.

Governing Equations

We wish to solve the inviscid flow equations, subject to certain jump conditions which model the effect of a screen on the flow. Nondimensional variables will be used in which the fluid density, screen half-height, and upstream velocity are unity. The resistance coefficient k determines the pressure drop across the screen $[P]$ through

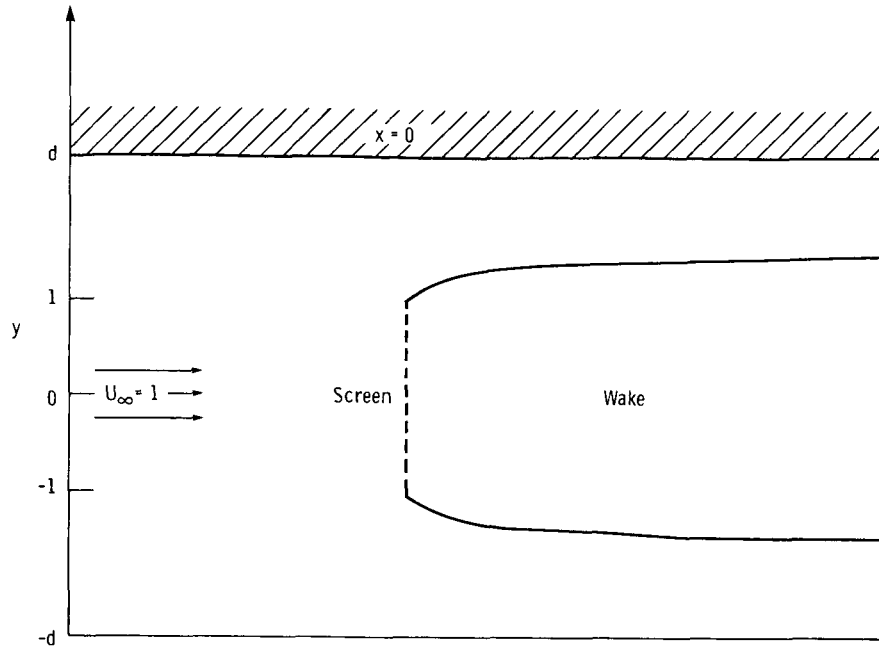$$[P] = \frac{1}{2} k U^2 \quad (x = 0, |y| < 1) \tag{1}$$

1

Figure 1.—Defining sketch of screen between two walls.

(ref. 1) where $U(x=0)$ is the velocity normal to the screen and the screen lies along $x=0$, $|y|<1$ (fig. 1). The tangential resistance coefficient B determines the jump in tangential velocity $[V]$:

$$[V] = BV_+ \qquad (2a)$$

where V_+ is the tangential velocity on the upstream side of the screen.
Mass conservation across the screen requires that

$$[U] = 0 \qquad (2b)$$

These jump conditions must be satisfied by solutions to the momentum and continuity equations:

$$\left. \begin{aligned} -\frac{\partial P}{\partial x} &= U\frac{\partial U}{\partial x} + V\frac{\partial U}{\partial y} \\[2mm] -\frac{\partial P}{\partial y} &= U\frac{\partial V}{\partial x} + V\frac{\partial V}{\partial y} \\[2mm] \frac{\partial U}{\partial x} &+ \frac{\partial V}{\partial y} = 0 \end{aligned} \right\} \qquad (3)$$

For flow confined by wind tunnel walls at $|y|=d$, an additional boundary condition is $V=0$ on the walls. The upstream condition is $U \to 1$, $V \to 0$ as $x \to -\infty$.

Approximate Analysis

In the next section an asymptotic analysis for $k \to ($ be done. Here a less formal approach is used, althou still is valid only when $k \ll 1$; it agrees with asymptotic analysis to $O(k)$. This approximate anal illustrates the general approach of this report.

Substituting $U = 1 + u$, $V = v$, and $H = P + 1/2 \ (u^2 +$ into equations (3) gives

$$\left. \begin{aligned} -\frac{\partial H}{\partial x} &= \frac{\partial u}{\partial x} - v\omega \\[2mm] -\frac{\partial H}{\partial y} &= \frac{\partial v}{\partial x} + u\omega \\[2mm] \frac{\partial u}{\partial x} &+ \frac{\partial v}{\partial y} = 0 \end{aligned} \right\} \qquad (4$$

Here $\omega = \partial v/\partial x - \partial u/\partial y$ is the vorticity, which vanishes outside of the wake. If ω is set identically to zero in equation (4), H satisfies Laplace's equation. Let R be the harmonic conjugate to H so that $H + iR$ is an analytic function in the complex plane cut along the screen. If B is set to zero, then $[H] = [P] = 1/2 \ kU^2 \ (0, |y| < 1)$ and $[R] = [V] = 0$ (see eq. (6)). Now, by the Plemelj formulas (ref. 4) and the boundary conditions to the problem, the analytic function $H + iR$ is found to be

$$H + iR = \frac{k}{16di} \int_{-i}^{i} U^2 \, (0, y'/i) \left[\cotanh \, \frac{\pi}{4d} \, (y' - z) \right.$$

$$\left. - \tanh \, \frac{\pi}{4d} \, (y' + z) - 2 \right] dy' \tag{5}$$

where $z = x + iy$. This satisfies $H \to 0$ as $x \to -\infty$ and $R = 0$ on $|y| = d$. The latter is required because, from equation (4) with $\omega = 0$ and the Cauchy-Riemann relations,

$$v = R \tag{6}$$

It turns out that $U(0, |y| < 1)$ is independent of y. If its value is denoted by U_s, equation (5) becomes

$$H + iR = \frac{kU_s^2}{4\pi i} \, \ln \left[\frac{\sinh \, \frac{\pi}{2d} \, (z - i)}{\sinh \, \frac{\pi}{2d} \, (z + 1)} \right] - \frac{kU_s^2}{4d} \tag{7}$$

where the branch cut of the logarithm is on the screen. Using equation (4) with $\omega = 0$ gives

$$U = -H + 1 - \frac{kU_s^2}{2} \, f(y) \tag{8}$$

where $f(y)$ is an arbitrary function of y, except for a possible jump across the screen. To satisfy equation (2b) and the upstream condition $U = 1$,

$$f(y) = \begin{cases} 0 & x < 0 \\ 0 & x > 0, \ |y| > 1 \\ 1 & x > 0, \ |y| \leq 1 \end{cases} \tag{9}$$

Hence, U is discontinuous across the wake boundary $(x > 0, |y| = 1)$, which is a vortex sheet of strength $1/2 \, kU_s^2$.

U_s is found by evaluating equation (8) on the screen, where $U = U_s$. Thus,

$$U_s = \frac{-2 + 2\sqrt{1 + k - (k/d)}}{k - (k/d)} \tag{10}$$

Equations (6) to (10) determine the flow field for given d and k. For instance, the drag coefficient for the screen is

$$C_D \equiv 2[P] = kU_s^2 \tag{11}$$

and far downstream the velocity is

$$1 + \frac{kU_s^2}{2d} \tag{12a}$$

outside the wake and

$$1 - \frac{1}{2} \, kU_s^2 \left(1 - \frac{1}{d} \right) \tag{12b}$$

inside the wake.

Expression (12a) agrees excellently with the data in figure 7 of Koo and James (ref. 2) where data extend to $k = 9$. Expression (12b) agrees with the data in their figure 8 up to $k = 3$, after which it falls below the data. Thus, when the present approximation is extended beyond its range of validity it gives wake velocities which are lower than observed. (Indeed, expression (12b) becomes negative at large k.) Equation (11) with $d = \infty$ is plotted as C_D versus k in figure 2, along with data transcribed from Graham (ref. 3). In cases where k was not measured, Graham used the formula $k = (\beta^{-2} - 1)$ to relate k to the screen open area ratio β. Laws and Livesey (ref. 5) state that the formula $k = 0.52 \, (\beta^{-2} - 1)$ is in better agreement with measurements; the latter formula was used in transcribing the data. Also shown in figure 2 are results from Koo and James' model and a Pade approximant to the two-term asymptotic expansion (see eq. (53)). For k greater than about 4 the flow through a screen becomes unstable and a recirculating wake may begin to form (Laws and Livesey, ref. 5). There is no basis for the present analysis at these higher values of k.

In the solution (8), the wake upper boundary is the line $y = 1$, $x > 0$. In the following asymptotic analysis, to lowest order, the wake rises above $y = 1$ a distance $s(x)$ given by

$$s(x) = \int_0^x V \, (x', y = 1) \, dx' =$$

$$- \frac{kU_s^2}{4\pi} \int_0^x \text{Re} \left[\ln \frac{\sinh \, \frac{\pi}{2d} \, x'}{\sinh \, \frac{\pi}{2d} \, (x' + 2i)} \right] dx' \tag{13}$$

Equations (6) and (7) were used to obtain V. When $d \to \infty$

$$\frac{s(x)}{kU_s^2} \to \frac{-1}{8\pi} \left(\ln \frac{x^2}{x^2 + 4} - 4 \, \text{Tan}^{-1} \frac{x}{2} \right) \tag{14}$$

In figure 3 $s(x)/kU_s^2$ is plotted for several values of d. Also shown are experimental data measured in the NASA Lewis 20 by 30 inch (Boy Scout) wind tunnel. In the experiments $d = 2$ and $k = 2.0$ and 0.6. Although the experimental wake boundary was very sharp initially, it became diffuse further downstream: the data indicate the height above the screen of the centerline of the shear layer. The data were normalized by the theoretical kU_s^2
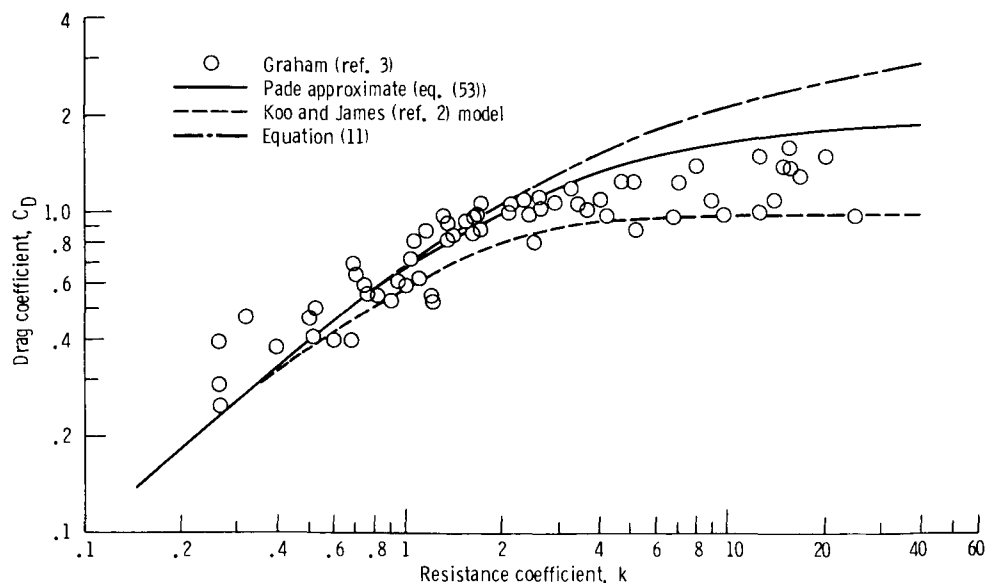
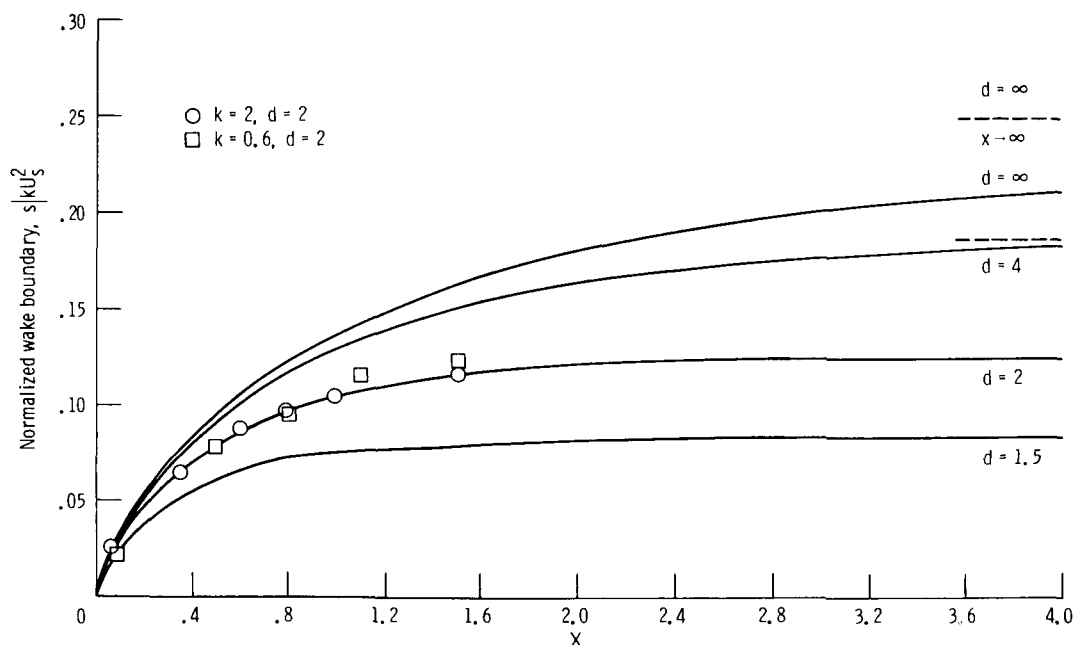Figure 2.—Drag coefficient as function of resistance coefficient.

Figure 3.—Wake boundary as computed from equation (13) for values of d indicated.

found from equation (10). It is seen that when $k < 2$ theory and experiment agree. The experiments were done in collaboration with Mr. D. McKinzie (NASA Lewis Research Center) in the initial phases of a study on shear flow instability.

Asymptotic Analysis

For this analysis we return to equations (1) to (3), and an expansion in powers of k is sought: for example,

$$U = U_0 + kU_1 + k^2 U_2 \dots$$

Also, B is assumed of the form

$$B = kB_1 + k^2 B_2 + k^3 B_3 \dots$$

Only the unbounded case, $d = \infty$, is treated. At lowest order

$$U_0 = 1, \quad P_0 = 0, \quad V_0 = 0$$

4

At order k, equations (1) to (3) become

$$\left.\begin{array}{l} \dfrac{-\partial P_1}{\partial x} = \dfrac{\partial U_1}{\partial x} \\[2mm] \dfrac{-\partial P_1}{\partial y} = \dfrac{\partial V_1}{\partial x} \\[2mm] \dfrac{\partial U_1}{\partial x} + \dfrac{\partial V_1}{\partial y} = 0 \end{array}\right\} \tag{15}$$

with $[U_1]=0=[V_1]$, $[P_1]=1/2$. Equations (15) are essentially the same as equations (4) with $\omega=0$. Their solution is found by letting $d \to \infty$ and setting $kU_s^2=1$ in equation (7):

$$P_1 + iQ_1 = \frac{-1}{4\pi i} \ln \left(\frac{z-1}{z+i} \right) \tag{16a}$$

and with equations (6) and (8)

$$U_1 - iV_1 = \frac{-1}{4\pi i} \ln \left(\frac{z-1}{z+i} \right) - \frac{1}{2} f(y) \tag{16b}$$

Note that this velocity is logarithmically singular at the edges of the screen. Hence, the expansion breaks down in a small region around the edges, order $e^{-1/k}$.

In equations (16) the screen wake lies in $x>0$, $|y|<1$, because $f(y)$ is nonzero there (eq. (9)). This representation of the wake would result in nonuniformity of the asymptotic expansion at the edge of the wake because $df/dy = -\text{sgn}(y)\, \delta(|y|-1)$. To avoid nonuniformity, we replace $f(y)$ by $f(y - \text{sgn}(y)\, s(x))$ with $s=ks_1 + k^2s_2 + k^3s_3 + \dots$, so that the upper boundary of the wake lies on $y = 1 + s(x)$. This does not affect the first order solution (16).

At order k^2, equations (1) to (3) become

$$\left.\begin{array}{l} \dfrac{-\partial P_2}{\partial x} = \dfrac{\partial U_2}{\partial x} + \dfrac{1}{2} \dfrac{ds_1}{dx} \left| \dfrac{\partial f}{\partial y} \right| + U_1 \dfrac{\partial U_1}{\partial x} + V_1 \dfrac{\partial U_1}{\partial y} \\[2mm] \dfrac{-\partial P_2}{\partial y} = \dfrac{\partial V_2}{\partial x} + U_1 \dfrac{\partial V_1}{\partial x} + V_1 \dfrac{\partial V_1}{\partial y} \\[2mm] \dfrac{\partial U_2}{\partial x} + \dfrac{\partial V_2}{\partial y} = 0 \end{array}\right\} \tag{17}$$

Taking

$$s_1 = \int_0^x V_1(x', y=1)\, dx'$$

removes the singularity (i.e., the δ-function associated with $\partial U_1/\partial y$) from the first of equations (17). Thus, s_1 is given by equation (14) with $kU_s^2=1$.

Now, if we let

$$H_2 = P_2 + \frac{1}{2}\left(U_1^2 + V_1^2 \right)$$

then equations (17) can be written

$$\left.\begin{array}{l} \dfrac{-\partial H_2}{\partial x} = \dfrac{\partial U_2}{\partial x} \\[2mm] \dfrac{-\partial H_2}{\partial y} = \dfrac{\partial V_2}{\partial x} + \dfrac{1}{2} U_1 \dfrac{\partial f}{\partial y} \end{array}\right\} \tag{18}$$

These equations indicate that $\nabla^2 H_2 = 0$ except for a jump across the vortex sheets of

$$\langle H_2 \rangle = \frac{1}{2} U_1(x, |y|=1)\, \text{sgn}(y)$$

The angled brackets denote a jump across the sheets. $U_1(x, |y|=1)$ is to be understood as the average of the velocities just above and just below $|y|=1$, so

$$\langle H_2 \rangle = -\left(\frac{1}{8} + \frac{1}{2} P_1(x,1) \right) \text{sgn}(y) \tag{19}$$

Again, it is convenient to introduce the harmonic conjugate to H_2, R_2; then from equations (18), $V_2 = R_2$. The jump of R_2 across the vortex sheets is found by removing a nonuniformity in the equations at next order (analogously to what was done with eqs. (17)). Doing so gives

$$U_1 \frac{ds_1}{dx} + \frac{ds_2}{dx} = V_2 + s_1 \frac{\partial V_1}{\partial y} = R_2 + s_1 \frac{\partial R_1}{\partial y}$$

on the upper vortex sheet ($y = 1$, $x > 0$). The jump of this equation is

$$\langle R_2 \rangle = \frac{ds_1}{dx} \langle U_1 \rangle = \frac{1}{2} V_1(x,1) = \frac{1}{2} Q_1(x,1) \tag{20}$$

where $ds_1/dx = V_1(x,1)$ has been used. Also on the lower sheet

$$\langle R_2 \rangle = \frac{1}{2} Q_1(x,1)$$

On the screen conditions (1) and (2) give

$$[H_2] = U_1(0,|y|<1) = -\frac{1}{4} \tag{21}$$

by using equations (16) and

$$[R_2] = B_1 Q_1(0,|y|<1) \tag{22}$$

Since $[P_2] = [H_2]$, to this order of approximation the pressure drag is uniformly spread over the screen.

A sectionally analytic function with jumps (eqs. (19) to (22)) is (Roos, ref. 4)

$$H_2 + iR_2 = \frac{1}{2\pi i}\left[\frac{1}{8}\ln\left(\frac{iz-1}{iz+1}\right) - \frac{1}{4}\ln\left(\frac{z-i}{z+i}\right)\right]$$

$$-\frac{1}{4\pi i}\int_0^\infty \frac{P_1(x',1) - iQ_1(x',1)}{x'-z-i}dx'$$

$$+\frac{1}{4\pi i}\int_0^\infty \frac{P_1(x',1) + iQ_1(x',1)}{x'-z+i}dx'$$

$$+\frac{B_1}{2\pi}\int_{-1}^1 \frac{iQ_1(0,y')}{iy'-z}dy' \tag{23}$$

To satisfy equation (2b) and the upstream condition U_2, $V_2 \to 0$:

$$U_2 + iV_2 = -H_2 - iR_2 + \frac{1}{4}f(y) \tag{24}$$

In equation (23) the first logarithm has branch cuts on the vortex sheets and the second is cut on the screen.

It follows from equation (23) that at this order of approximation U is not constant on the screen; hence, the approximate analysis of the previous section breaks down. Also, since

$$[P_3] = \frac{1}{2} U_1^2(0,|y|<1) + U_2(0,|y|<1) = \frac{1}{32} + U_2 \tag{25}$$

and U_2 is a function of y on the screen, at third order the pressure drag is no longer uniformly distributed. This y-dependence of U_2 is produced by wake vorticity and by the tangential drag on the screen.

It follows from equation (25) and the preceding method of analysis that at third order the downstream velocity inside the wake is

$$U_3(\infty,y) = -[P_3] - U_1(\infty,y)U_2(\infty,y)$$

$$= \frac{3}{32} - U_2(0,y) \tag{26}$$

for $y<1$. Hence, the velocity is nonuniform within the wake or, in other words, vorticity is distributed throughout the wake.

The total third-order drag coefficient of the screen is

$$C_{D_3} = \int_{-1}^1 [P_3]\,dy = \frac{1}{16} + \int_{-1}^1 U_2(0,y)\,dy$$

$$= \frac{1}{16} - \int_{-1}^1 H_2(x\uparrow 0,y)\,dy \tag{27}$$

Substituting equation (16a) into equation (23) shows that the integrals required to evaluate equation (27) can be done in closed form. The result is

$$C_{D_3} = \frac{5}{48} - \frac{B_1}{8\pi^2}\left(-4(\ln 2)^2 + \frac{4\pi^2}{3} - 8\sum_{n=1}^\infty \frac{1}{2^n n^2}\right) \tag{28}$$

Thus, to third order,

$$C_D = k - \frac{k^2}{2} + \frac{5k^3}{48} - 0.0833B_1 k^3 \tag{29}$$

The net *tangential* drag on half the screen is

$$\int_0^1 U(0,y)[V]\,dy = \int_0^1 k^2[V_2] + k^3 U_1[V_2] + k^3[V_3]\,dy$$

to third order. Using equation (2a) gives

$$[V_3] = B_2 V_{1+} + B_1 V_{2+}$$

Using equations (23) and (24) for V_{2+} gives

$$\int_0^1 U[V]\,dy = \left[k^2 B_1 + k^3\left(B_2 + \frac{1}{2}B_1^2 - \frac{1}{4}B_1\right)\right]\frac{\ln 2}{2\pi} \tag{30}$$

This is the tangential drag on a screen adjacent to a plane wall.

Unsteady Flow

The present approach can be applied to unsteady flow through a screen. Turbulent flow through a screen was analyzed by Graham (ref. 3). Here we consider an easier problem in which the unsteadiness is due to uniform pulsations of the flow. The governing equations (3) now have $\partial U/\partial t$ and $\partial V/\partial t$ added to their right sides. The jump conditions (1) and (2) are assumed to remain valid at the frequency of interest.

The pulsating flow will be taken as

$$U_0 = 1 + \alpha \cos \omega t \tag{31}$$

with $\alpha < 1$. Then, at $O(k)$

$$\left. \begin{array}{l} \dfrac{-\partial P_1}{\partial x} = U_0 \dfrac{\partial U_1}{\partial x} + \dfrac{\partial U_1}{\partial t} \\[3mm] \dfrac{-\partial P_1}{\partial y} = U_0 \dfrac{\partial V_1}{\partial x} + \dfrac{\partial V_1}{\partial t} \\[3mm] \dfrac{\partial U_1}{\partial x} + \dfrac{\partial V_1}{\partial y} = 0 \end{array} \right\} \tag{32}$$

with $[P_1] = 1/2 U_0^2$ and U_1, $V_1 \to 0$ as $x \to -\infty$. As in equation (16a)

$$P_1 = U_0^2 \left[\frac{1}{4\pi} \left(\text{Tan}^{-1} \frac{x}{y-1} - \text{Tan}^{-1} \frac{x}{1+y} \right) \right] \tag{33}$$

with U_0 given by equation (31). It is convenient to rewrite this as

$$P_1 = \sum_{m=-2}^{2} e^{im\omega t} \left(\frac{\alpha}{2} \right)^{|m|} \sum_{n=0}^{1} \psi_{mn} \left(\frac{\alpha}{2} \right)^{2n} \widetilde{\psi}(x) \tag{34}$$

where $\widetilde{\psi}$ is the term in brackets in equation (33), with the y-argument suppressed. Comparing equation (34) with equation (33) gives

$$\psi_{-mn} = \psi_{mn}, \ \psi_{00} = 1, \ \psi_{10} = \psi_{01} = 2, \ \psi_{20} = 1$$

and all other ψ_s's equal zero.

A solution to equation (32) will be sought in the form

$$U_1 = \sum_{m=-\infty}^{\infty} e^{im\omega t} \left(\frac{\alpha}{2} \right)^{|m|} \sum_{q=0}^{\infty} \left(\frac{\alpha}{2} \right)^{2q} \phi_{mq}(x) \tag{35}$$

Substituting this and equation (31) into equation (32) and equating coefficients of $\alpha^n e^{im\omega t}$ give

$$-\left(\phi'_{m+1,q-1} + \phi'_{m-1,q} + \psi_{mq} \widetilde{\psi}' \right) = \phi'_{mq} + im\omega \phi_{mq} \tag{36}$$

for $m > 0$, where primes denote differentiation with respect to x. For $m = 0$,

$$\phi_{0q} = -\psi_{0q} \widetilde{\psi} - 2\phi_{1,q-1} \tag{37}$$

and ϕ_{mq} can be found by solving equation (36) recursively in q.

When $q = 0$, because $\phi_{m,-1} = 0$, equation (36) becomes

$$-\phi'_{m-1,0} - \psi_{m0} \widetilde{\psi}' = \phi'_{m0} + im\omega \phi_{m0} \tag{38}$$

Let

$$\widetilde{\phi}'(x;\Omega) + i\Omega \widetilde{\phi} = -\widetilde{\psi}' \tag{39}$$

where $\widetilde{\phi}' \to 0$ as $x \to -\infty$; that is,

$$\widetilde{\phi}(x;\Omega) = e^{-i\Omega x} \left[\int_{-\infty}^{x} e^{i\Omega x'} \widetilde{\psi}(x') \, dx' + g(y) \right] \tag{40}$$

The function $g(y)$ is determined by condition (26) and is zero outside the wake. Then a solution to equation (38) can be found as

$$\left. \begin{array}{l} \phi_{m0}(x) = \displaystyle\sum_{r=1}^{m} A_r^m \widetilde{\phi}(x;r\omega) \qquad m > 0 \\[4mm] \phi_{00} = -\widetilde{\psi}(x) \end{array} \right\} \tag{41}$$

Clearly, $A_1^1 = 1$. Substituting equations (39) and (41) into equation (38) and equating the coefficients of $\widetilde{\psi}'$ and $\widetilde{\phi}(r\omega)$ to zero yield

$$\left. \begin{array}{l} A_r^m = -\dfrac{r}{(m-r)} A_r^{m-1} \qquad r < m \\[4mm] \displaystyle\sum_{r=1}^{m} A_r^m = -\psi_{m0} + \sum_{r=1}^{m-1} A_r^{m-1} \end{array} \right\} \tag{42}$$

The right side of this last equation is 0 when $m = 2$. Hence, it follows that

$$\sum_{r=1}^{m} A_r^m = 0 \qquad m \geq 2 \tag{43}$$

Using equations (42) and (43) gives

$$A_r^m = \frac{r^m}{(m-r)!} \, a_r \tag{44}$$

with $a_1 = 1$ and

$$a_m = -\frac{1}{m^m} \sum_{r=1}^{m-1} \frac{r^m a_r}{(m-r)!}$$

which completes the solution with $q = 0$.

When $q = 1$, equation (36) becomes

$$-\phi'_{m+1,0} - \phi'_{m-1,1} = \phi'_{m,1} + im\omega\phi_{m,1} \tag{45}$$

for $m > 0$. $\phi_{m+1,0}$ is given by equation (41). A solution to equation (45), using equation (37), is found readily in terms of $\widetilde{\phi}(x;\Omega)$ and $\partial\widetilde{\phi}(x;\Omega)/\partial\Omega$. The latter, which is abbreviated to $\partial\widetilde{\phi}$, satisfies

$$\partial\widetilde{\phi}' + i\Omega \, \partial\widetilde{\phi} = -i\widetilde{\phi} \tag{46}$$

Assuming

$$\phi_{m,1} = \sum_{r=1}^{m+1} B_r^m \widetilde{\phi}(x;\omega) + C_m\omega \, \partial\widetilde{\phi}(x;\omega) \tag{47}$$

and equating coefficients of $\widetilde{\phi}(r\omega)$, $\partial\widetilde{\phi}$, and $\widetilde{\psi}$ in equation (45) to zero give

$$C_m = \frac{1}{(m-1)!}$$

For $r > 1$,

$$\left.\begin{array}{ll} B_r^m = -rA_r^{m+1} & r \neq m \\[3em] B_m^m = -B_{m+1}^m - \displaystyle\sum_{r=1}^{m-1} B_r^m & r = m, \ B_1^1 = -2, \ B_2^1 = 2 \end{array}\right\} \tag{48a}$$

For $r = 1$ and $m > 1$

$$B_1^m = \frac{C_{m-1} + C_m + B_1^{m-1} + A_1^{m+1}}{m-1} \tag{48b}$$

The B_1^m can be determined recursively. Solutions for higher values of q are found similarly.

As $x \to \infty$, $\partial\phi/\phi \to \infty$, so the expansion (35) is nonuniform in x. However, it is easily renormalized: equations (41) and (47) can be combined as

$$\phi_m \equiv \sum_{q=0}^{\infty} \left(\frac{\alpha}{2}\right)^{2q} \phi_{mq} = A_1^m \widetilde{\phi}\left[\omega\left(1 + \frac{\alpha^2 C_m}{A_1^m}\right)\right]$$

$$+ \sum_{r=2}^{m} A_r^m \widetilde{\phi}(r\omega) + \frac{\alpha^2}{4} \sum_{r=1}^{m+1} B_r^m \widetilde{\phi}(r\omega) + O(\alpha^4) \tag{49}$$

with the x and y dependence suppressed. This form for the first term on the right side removes the nonuniformity.

The preceeding solution for U_1 enables one to calculate the unsteady drag on the screen to $O(k^2)$.

The pressure jump at second order is

$$[P_2] = U_0 U_1 = \sum_{m=-\infty}^{\infty} \left(\frac{\alpha}{2}\right)^{|m|} \left(\phi_m + \frac{\alpha}{2}\phi_{m-1}\right.$$

$$\left.+ \frac{\alpha}{2}\phi_{m+1}\right)\bigg|_{x=0} e^{im\omega t} \tag{50}$$

by having used equations (31) and (35) with ϕ_m defined by equation (49). This pressure is not constant on the screen, so the nonuniform drag occurs at lower order than in the steady case and is not due to wake effects.

The second-order drag is determined by integrating equation (50) over the screen:

$$D_2 = \sum_{m=-\infty}^{\infty} \left(\frac{\alpha}{2}\right)^{|m|} D_2^m e^{im\omega t} \tag{51}$$

with

$$D_2^m = \int_{-1}^{1} \phi_m(0,y') + \frac{\alpha}{2}\phi_{m-1}(0,y') + \frac{\alpha}{2}\phi_{m+1}(0,y') \, dy'$$

From equation (40) with equation (33) for $\widetilde{\psi}(x,y)$,

$$\hat{\phi}(\Omega) \equiv \int_{-1}^{1} \widetilde{\phi}(0,y;\Omega) = \frac{\cosh 2\Omega - 1}{2\pi i\Omega}(\gamma + \ln 2i\Omega) - \frac{\sinh 2\Omega}{4\Omega}$$

$$+ \frac{\cosh 2\Omega}{2\pi i\Omega}\left\{\text{chi } 2\Omega - \gamma - \ln 2i\Omega\right\} + \frac{\sinh 2\Omega}{2\pi\Omega} \text{ shi } 2\Omega \tag{52}$$

where shi and chi are the sinh and cosh integrals and γ is Euler's constant (Abramowitz and Stegun, ref. 6). The term D_2^m can be evaluated using equations (49) and (52) in equation (51). In particular, the term linear in α is

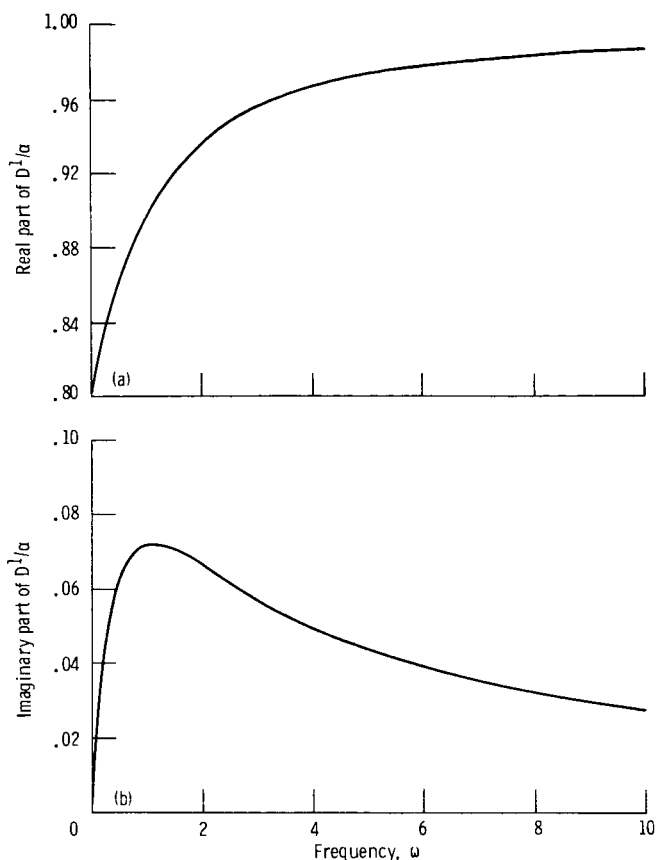$$\frac{1}{2}D_2^1 = \frac{1}{2}\,\hat{\phi}(\omega) + O(\alpha)$$

To second order, $D + kD_1 = k^2 D_2$. Since $[P_1] = 1/2\ U_0^2$, $D_1 = U_0^2$. In the steady case, the Pade approximant

$$D = \frac{kD_1}{1 - (kD_2/D_1)} = \frac{k}{1 + \frac{1}{2}k} \qquad (53)$$

fits experimental data quite well (fig. 2). Thus, it seems sensible to write

$$\frac{D^1}{\alpha} = \frac{k}{\left[1 - \dfrac{k\,\hat{\phi}(\omega)}{2}\right]} + O(\alpha) \qquad (54)$$

for the unsteady drag at frequency ω. In figure 4 the real and imaginary parts of D^1/α are plotted against ω with $k = 1$, and in figure 5, $|D^1\alpha|$ is plotted for $k \le 4$ with $\omega = 0.1$, 1, and 10.

(a) Real parts of D^1/α.

(b) Imaginary part of D^1/α.

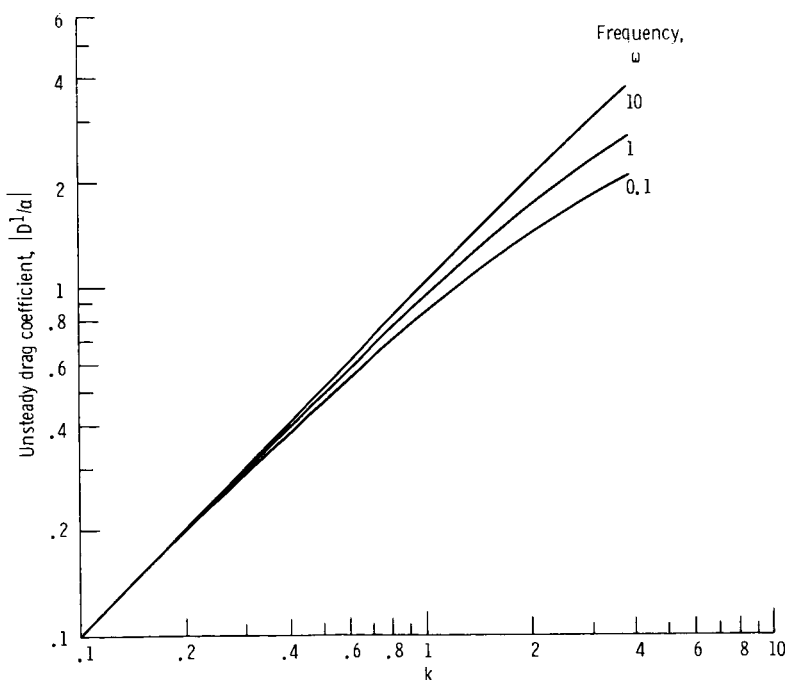Figure 4.—Unsteady drag coefficient as function of frequency ω with $k = 1$.

Figure 5.—Unsteady drag coefficient as function of k with frequency $\omega = 0.1$, 1, and 10.

Concluding Remarks

A method for calculating steady or unsteady flow through very porous screens has been described. Good correspondence is found between theory and experiment by carrying out the asymptotic expansions to second order and using Pade approximants. Muramoto and Durbin have applied the present method to flow through inclined screens (paper submitted to AIAA 18th Fluid Dynamics and Plasma Dynamics and Lasers Conference, July 1985). In this case distributed wake vorticity appears at second order in the asymptotic expansion; the theoretical wake velocity profile is found to be in agreement with experimental data.

Lewis Research Center
National Aeronautics and Space Administration
Cleveland, Ohio, December 18, 1984

References

1. Abramowitz, Milton; and Stegun, Irene A.: Handbook of Mathematical Functions. Dover, 1965.
2. Graham, J.M.R.: Turbulent Flow Past a Porous Plate. J. Fluid Mech., vol. 73, Part 3, Feb. 10, 1976, pp. 565–591.
3. Koo, J.-K.; and James, David F.: Fluid Flow Around and Through A Screen. J. Fluid. Mech., vol. 60, Part 3, Sept. 18, 1973, pp. 513–538.
4. Laws, E.M.; and Livesey, J.L.: Flow through Screens. Ann. Rev. Fluid Mech. vol. 10, 1978, pp. 247–266.
5. Roos, Bernard W.: Analytic Functions and Distributions in Physics and Engineering. Wiley, 1969.
6. Taylor, G.I.: Air Resistance at a Flat Plate of Very Porous Material. The Scientific Papers of G.I. Taylor, Vol. III, G.K. Batchelor, ed., Cambridge Univ. Press, 1944, p. 383.

1. Report No. NASA TP-2436	2. Government Accession No.	3. Recipient's Catalog No.
4. Title and Subtitle Flow Through Very Porous Screens		5. Report Date March 1985
		6. Performing Organization Code 505-31-3B
7. Author(s) Paul A. Durbin and Kenneth K. Muramoto		8. Performing Organization Report No. E-2360
		10. Work Unit No.
9. Performing Organization Name and Address National Aeronautics and Space Administration Lewis Research Center Cleveland, Ohio 44135		11. Contract or Grant No.
		13. Type of Report and Period Covered Technical Paper
12. Sponsoring Agency Name and Address National Aeronautics and Space Administration Washington, D.C. 20546		14. Sponsoring Agency Code

15. Supplementary Notes

16. Abstract

An asymptotic analysis is done for flow through and around screens with small resistance coefficient. Both steady and oscillatory flows are considered, but only the case of a screen normal to the flow is treated. At second order in the asymptotic expansion the steady flow normal to the screen is nonuniform along the screen, due to components induced by the wake and by tangential drag. Therefore, the third-order pressure drop is nonuniform and the wake contains distributed vorticity, in addition to the vortex sheet along its boundary. The unsteady drag coefficient is found as a function of frequency.

17. Key Words (Suggested by Author(s)) Screens Resistance coefficient Drag	18. Distribution Statement Unclassified - unlimited STAR Category 34		
19. Security Classif. (of this report) Unclassified	20. Security Classif. (of this page) Unclassified	21. No. of pages 12	22. Price* A02

National Aeronautics and
Space Administration

Washington, D.C.
20546

Official Business
Penalty for Private Use, $300

THIRD-CLASS BULK RATE

NASA

POSTMASTER: If Undeliverable (Section 158
                Postal Manual) Do Not Return